Volume 1 | Number 1 | Jan 2013 | Pages 1–100

This is an *Accepted Manuscript*, which has been through the Royal Society of Chemistry peer review process and has been accepted for publication.

Accepted Manuscripts are published online shortly after acceptance, before technical editing, formatting and proof reading. Using this free service, authors can make their results available to the community, in citable form, before we publish the edited article. We will replace this *Accepted Manuscript* with the edited and formatted *Advance Article* as soon as it is available.

You can find more information about *Accepted Manuscripts* in the **Information for Authors**.

Journal Name

Nanoscale

ARTICLE TYPE

Tailored synthesis of hierarchical spinous hollow titania hexagonal prisms via a self-template route

Ye Zhang,[a] Buyuan Guan,[a] Duihai Tang,[b] Xue Wang,[a] Tao Wang,[a] Bo Zhi,[a] Dongmei Wang,[a] Xiang Li,[a] Yunling Liu[a] and Qisheng Huo*[a]

Novel hierarchical spinous hollow titania hexagonal prisms are prepared through a facile fluorine-free self-template route by using $Ti_2O_3(H_2O)_2(C_2O_4) \cdot H_2O$ (TC) hexagonal prisms as precursor. The hollowing transformation can be elucidated by the template-free Kirkendall effect, and diverse nanostructures can also be synthesized during the conversion process, such as the spinous core-shell and yolk-shell nanocomposites. The hierarchical hollow microparticles are composed of ultrathin nanobelts with 50~100 nm in length and about 10 nm in thickness, and possess a higher surface area of up to 163 $m^2 g^{-1}$ compared with solid microparticles (49 $m^2 g^{-1}$). This type of morphology is of great interest for lithium-ion batteries because of its shorter length for Li^+ transport and better electrode–electrolyte contact.

Introduction

Recently, hollow structure materials[1,2] are receiving more and more attention for their excellent properties in the fields ranging from catalysis[3,4] to energy storage[5] and biomedical engineering.[6-8] A variety of synthesis approaches[9] have been developed to generate hollow structures, such as the conventional hard[10] and soft templating methods.[11,12] Rattle-type V_2O_5 hollow microspheres have been successfully fabricated by using carbon colloid spheres as hard template.[13] Wang's group has reported the preparation multishelled Cu_2O hollow spheres by using the CTAB micelles and vesicles as template.[14] Moreover, a novel self-template route[15] based on Kirkendall effect,[16,17] Ostwald ripening,[18,19] "surface-protected etching"[20] or galvanic replacement[21] has emerged, which is more controllable and become popular.

Among various inorganic materials, titania[22,23] has triggered great enthusiasm for its promising applications in "energy"[24-29] and "environmental" areas.[30-32] Titania is an attractive anode material for lithium-ion batteries for its naturally available, inexpensive, and environmental benignity. Compared with the conventional graphite, a relative high intercalate Li^+ potentials (1.7V versus Li/Li^+) can avoid the occurrence of lithium dendrites on the electrode under high-rate charge/discharge and address the safety issue.[33-35]

Significant efforts have been dedicated to the synthesis of diverse hollow titania materials with different sizes, shapes and polymorphs due to the advantages of hollow micro/nanostructures.[30,35-40] By target etching of amorphous hydrous solid spheres, Wang et al. have successfully synthesized a large scale urchin-like mesoporous TiO_2 hollow spheres composed of 1D single crystal anatase nanothorns with exposed {101}facets.[41] Caruso et al .have developed a facile fluorine-free process to prepare anatase nanostructures with complicate morphologies.[42] Monodisperse TiO_2 hierarchical hollow microspheres assembled by nanospindles have been reported by Xu et al., the size of which could be tuned by adjusting the ammonia content in the precursor solution.[43] There are only a few reports on the fabrication of hierarchical hollow titania architectures, moreover all of above materials possess spherical morphology. Thus it is still a great challenge to prepare nonspherical hierarchical hollow particles to date.

Herein we have successfully fabricated hierarchical spinous hollow TiO_2 hexagonal prisms via a self-template route in the solvothermal process and investigated their performance of lithium-ion storage. $Ti_2O_3(H_2O)_2(C_2O_4) \cdot H_2O$ (TC) hexagonal prisms are prepared as the designed precursor. Through a facile solvothermal process, the precursor will undergo two different transitions into core/shell nanostructure first and then yolk/shell, which will be converted to hierarchical hollow titania structure eventually. The as-synthesized hierarchical hollow TiO_2 sample not only maintains the original morphology, but also possesses a high surface area up to 163 $m^2 g^{-1}$ after calcination. The calcined hierarchical hollow material exhibits well electrochemisty properties when used as an anode for lithium ion batteries.

Experimental Section

Chemicals: $TiOSO_4 \cdot xH_2SO_4 \cdot xH_2O$ was purchased from Aladdin. $Li_2C_2O_4$ was obtained from Energy Chemical. Butyl alcohol and ammonia (28wt% aqueous solution) were purchased from Beijing chemical works without further purification. Ultrapure water (resistivity>18.2MΩ cm)

Preparation of $Ti_2O_3(H_2O)_2(C_2O_4) \cdot H_2O$ (TC).

Titanium oxalate-based compound, $Ti_2O_3(H_2O)_2(C_2O_4) \cdot H_2O$, TC, was chosen as precursor, which was synthesized by using the method described in the reported work.[44] 1.35g of

$TiOSO_4 \cdot xH_2SO_4 \cdot xH_2O$ and 0.675g of $Li_2C_2O_4$were dissolved in 30 ml of warm water. The clear solution obtained was transferred to a 120 ml plastic bottle, which was treated at 85 °C for 3 h under static condition. The white power was collected by centrifugation (5000rpm) and then washed with water until no SO_4^{2-}residue.

Synthesis of hierarchical spinous hollow titania hexagonal prisms (SHTHPs)

In a typical synthesis, 0.036g of TC was dispersed in 6 ml of butyl alcohol, and 0.1 ml of ammonia was then added into the suspension. The resulting mixture was transferred into a 23 ml Teflon-lined autoclave and heated at 160 °C for 20 h. The white product was collected by centrifugation, washed several times with deionized water, and dried in an oven at 65 °Covernight. The dried powder was named as SHTHPs, and then it was calcined at 450 °C in air for 2 h with a heating ramp of 5 °C min^{-1} to obtain better crystalized titania and remove organic remains in the sample. Solid titania was obtained from the TC under the same calcination conditions.

Material characterizations

The X-ray diffraction (XRD) data of powder were collected on a Rigaku D/Max 2550 X-ray diffractometer using CuKa radiation (λ = 1.5418 Å) operated at 200 mA and 50 kV. The images of the products were recorded on scanning electron microscopy (SEM) 5 kV transmission electron microscopy (TEM) using an FEI Tecnai G^2 F20s-twin D573 transmission electron microscopeoperating at 200 kV. N_2 adsorption–desorption isotherms were determined at 77 K via MicromeriticsTristar 2420 analyzer. The infrared (IR) spectra were obtained via Bruker IFS 66V/S FTIR spectrometer using KBr pellets. The thermogracimetric analysis (TGA) was performed with a heating ramp of 10 °C min^{-1} in a flow of air. XPS (X-ray photoelectron spectroscopy) data was obtained on a Thermo ESCALAB 250 operated at 15 kW (mono chromatic Al-Ka radiation, 1486.6 eV).

Electrode preparation and electrochemical characterization

The electrochemical measurements of the solid titania and hollow materials were carried out using CR2032 coin type cells with lithium metal as the counter and reference electrodes at room temperature. 1 M LiPF6 in a 50:50 w/w mixture of diethyl carbonate and ethylene carbonate was selected as electrolyte. In order to fabricate the working electrode the samples, carbon black as conductive material, and polyvinylidene fluoride as binder in amass ratio of 8:1:1were mixed together homogeneously. Then the slurry was spread on a copper foil current collector and dried at 120 °C for 20 h. The cells were constructed in an argon-filled glove box with the concentrations of moisture and oxygen at below 1 ppm. The capacity of the electrode was measured using Neware Cell tester in the voltage range of 1-3 V.

Results and discussion

Synthesis and characterization of the hierarchical spinous hollow structures

The XRD pattern of the TC, $Ti_2O_3(H_2O)_2(C_2O_4)\cdot H_2O$, in Fig. S1†was consistent with the previous reported results.[44,45] Fig. 1a and b showed the SEM and TEM images of the TC which was consisted of uniform monodisperse particles having hexagonal prism morphology with a side length ranging from 0.7 to 1.6 μm and a thickness of about 0.5 μm. A close observation to the microstructure revealed that the particles possessed extremely smooth surfaces. The hierarchical spinous hollow titania hexagonal prisms (SHTHPs) were prepared by treating the TC in a butyl alcohol and ammonia solution at 160 °C for 20 h. The hollow interiors were demonstrated by some broken microparticles and could be further verified by TEM analysis (Fig. 1c and d). As shown in Fig. 1d (inset), the spinous surfaces of the hollow microparticles were composed of ultrathin nanobelts with 50~100 nm in length and about 10 nm in thickness. According to the XRD patterns in Fig. S1†, the diffraction peaks of the precursor disappeared after solvothermal treatment 20 h and some new broad peaks showed up, indicating the complete conversion of the TC to titania. We have randomly selected 150 entities to analysis the monodispersion of TC and SHTHPs respectively, and the histograms representing the side length population of the particles were shown in Fig. S2†.Upon calcination in air at 450 °C for 2 h, the morphologies of the TC and the SHTHPs were preserved (Fig. 1e-h). Time-dependent experiments were carried out to investigate the system change over time. The composition evolution from TC solution to SHTHPs was identified by IR spectrum and XRD data. As shown
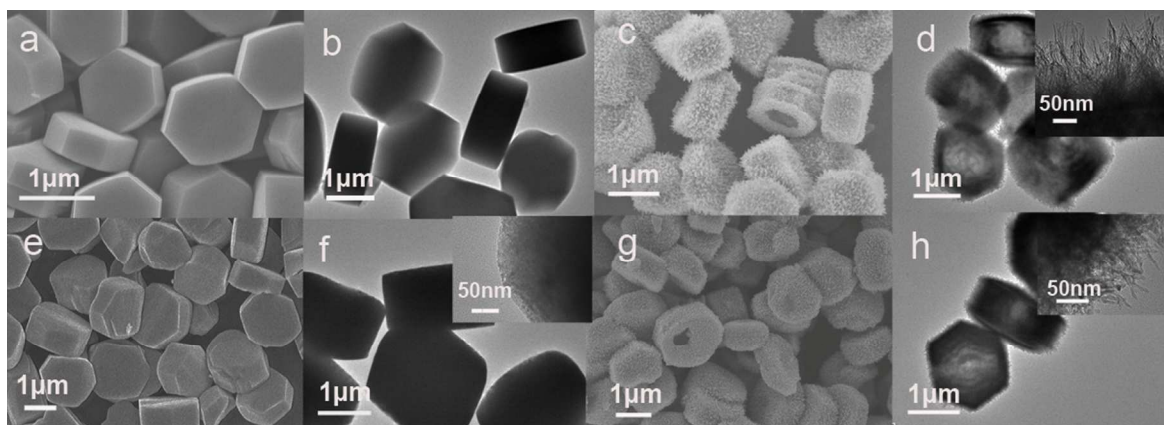

Fig. 1 SEM and TEM images of the solid and hollow microparticles: (a and b) TC, (c and d) SHTHPs, (e and f) solid titania, (g and h) calcined SHTHPs
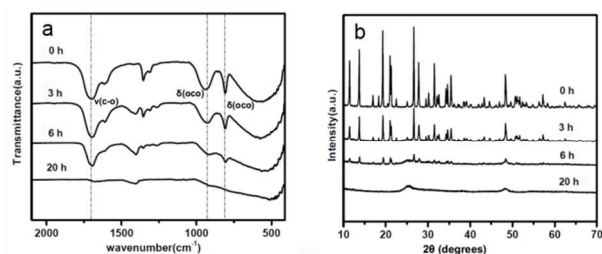
Fig.2 IR spectrums (a) and XRD patterns(b) of the products obtained after solvothermal treatment.

Fig.3 XRD pattern (a) and N_2adsorption-desorption isotherms (b) of the solid titania and calcined SHTHPs.

in the IR spectra (Fig. 2a), The ν (c-o) at 1697 cm^{-1} and δ (o-c-o) vibrations at 941 and 808 cm^{-1} indicated the existence of organic bands related to the oxalate anions. During the solvothermal process, the intensity of these absorption bands became weaker and disappeared after 20 h. The XRD patterns demonstrated the corresponding changes of these samples (Fig. 2b).The appearance of the obvious broad diffraction peak around 2θ = 25.6° could indicate the formation of titania, which was associated with the nanobelts on the surfaces of microparticles. Progressively, this peak was more intensive along with the increase of reaction time. At length all the diffraction peaks of the TC disappeared, and the result revealed that the final product was just consisted of a poorly crystallized TiO_2. As shown in Fig. 3a, the calcined materials both exhibited X-ray peaks of anatase TiO_2 (ICCD card No.21-1272), and the SHTHPs showed better crystallization after calcination. The broad diffraction peaks of the hierarchical hollow material indicated that the size of the primary TiO_2 crystals in calcined SHTHPs was smaller than those in the solid titania (calcined TC) according to Scherrer equation,[46] and the TEM images in Fig. 1f and h (inset) could also confirmed this result. The primary particles in solid titania aggregated together and the borders between them were not clear. Fig. 3b presented the nitrogen adsorption–desorption isotherms of these materials after calcination. The result revealed that the BET surface area of the calcined SHTHPs was 163 m^2 g^{-1},higher than that of solid titania (49 m^2 g^{-1}).It could also be observed that the hierarchical

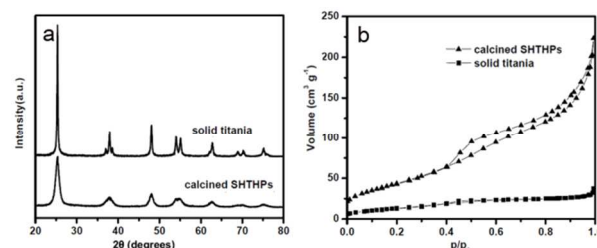hollow material exhibited a characteristic inkbottle-type IV isotherm with an obvious hysteresis loop, derived from the mesopores among nanobelts and the large void space in the hollow interiors. Thermograimetry (TG) was performed to investigate the thermal behaviour of SHTHPs during calcination. As displayed in Fig. S3†, there was small weight loss over 450 ^{o}C, indicating that almost all the organic remains have been removed after calcination. XPS analysis was carried out to investigate the surface composition of calcined SHTHPs (Fig. S4†). No signal around 400 eV was detected, indicating that there was no N-doping in the hierarchical hollow material.[47]

Moreover, products synthesized at varied intervals were examined by SEM and TEM observation. As shown in Fig. 4b and Fig. S5†, after solvothermal treatmentat 160 ^{o}C for 3 h core-shell nanostructured hexagonal prisms appeared, covered with ultrathin nanobelts. By prolonging the solvothermal time to 6h, a yolk-shell structure was obtained (Fig. 4c and Fig. S5†). The TEM images showed the detailed features of the microparticles which had about 300 nm thick shells consisting of numerous nanobelts. Further increasing the solvothermal treatment time to 20 h, well defined spinous hollow hexagonal prisms formed with an inner cavity of about 1 μm in length.

Formation mechanism and the effects of reaction parameters

Based on the above experimental results and analysis, a conceivable synthetic route was raised, which was schemed in Fig. 4e. The successful fabrication of the spinous hierarchical
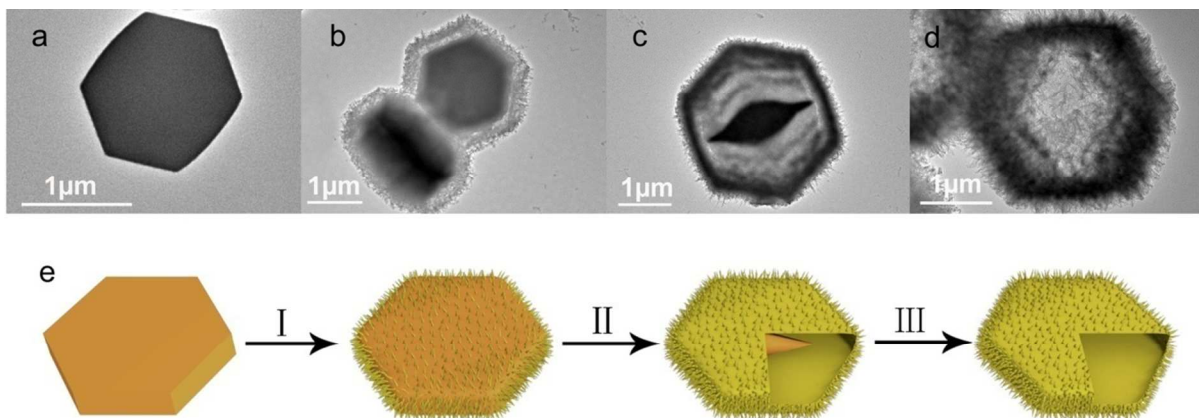

Fig.4 SEM and TEM images of the TChexagonal prisms (a) and products obtained with different solvothermal durations: (b) 3h for TC@titania core-shell structure, (c) 6h for TC@titania yolk-shell structure, (d) 20h for hollow titania structure. (e) Formation process of hierarchical spinous hollow titania hexagonal prisms.
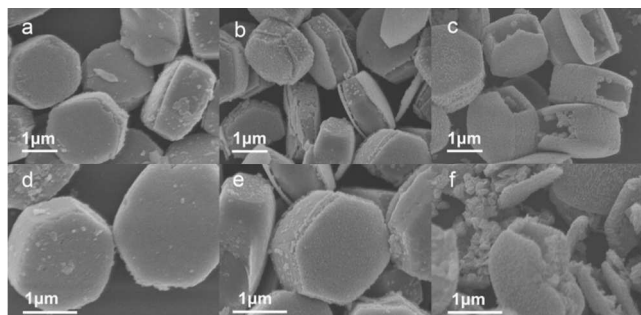
Fig.5 SEM images of the products prepared by replacing ammonia with water under otherwise identical conditions for 3h (a and d), 6 h (b and e) and 20h (c and f).

$$Ti_2O_3(H_2O)_2(C_2O_4) + H_2O \xrightarrow{\text{Butanol}} 2TiO_2 + 3H_2O + H_2C_2O_4 \quad (1)$$

hollow titania material mainly included three steps: (I)In the butyl alcohol and ammonia solution, the conversion of the TC was conducted on the surface of the microparticles at the initial stage. The exterior part of the microparticles was converted into titania and exhibited a core-shell structure. (II) The interior part gradually participated in the reaction and the Kirkendall effect,[16,17,48] occurred, giving rise to the yolk-shell nanostructure with increased reaction time. (III) After reacting 20h, all the microparticles were converted into spinous hollow hexagonal prisms completely eventually.

In the presence of a small amount of water, the hydrolysis of the TC was first conducted in (I), and subsequently Ti-O-Ti network would form through the condensation of the hydrolysis product (eq1).In order to investigate the formation process further, especially the special spinous surface morphology structure, a control experiment was designed, which was performed only by replacing ammonia with pure water. Ammonia was found to serve as the shape controller and reaction accelerator in the present synthesis system. As revealed by SEM analysis (Fig. 5), when ammonia was absent, the products retained the parent morphology after reaction 3 h and 6 h, but their surface become rough. The hollow structure could also be obtained after 20h, however, different from that in the presence of ammonia. Ammonia in our synthesis system played the important role in the growth of spinous surface feature for its strong affinity to the surface titanium ion of the crystalline TiO_2 particles.[49] According to the XRD result shown in Fig. S6†, the TC was almost converted to titania after 10h in the presence of ammonia. However, without ammonia there was still some TC residue. The above analysis indicated that ammonia was essential in the solvothermal process.

Electrochemical Characterization

In order to evaluate the lithium storage properties of solid titania and calcined SHTHPs, the electrochemical tests were conducted with the standard TiO_2/Li half-cell configuration. The electrochemical performance of the solid and hollow materials was shown in Fig. 6. The variation in discharge capacities of them at different rate have been studied (Fig. 6a). The value decreased when increasing the current density, which was
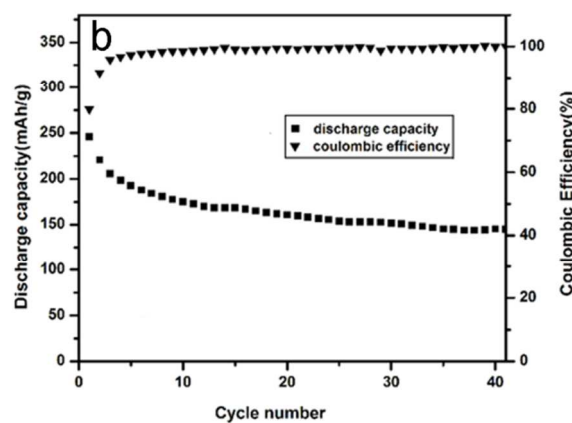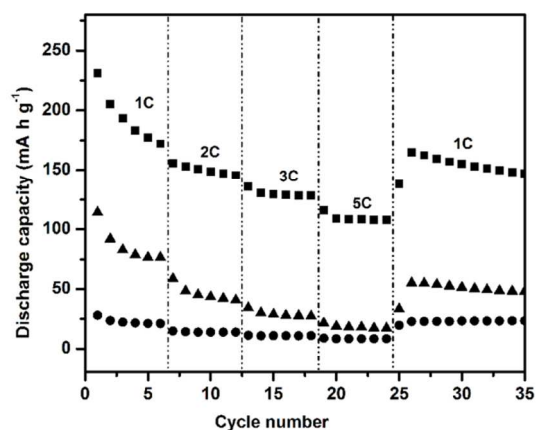

Fig. 6 (a) Rate capability of solid titania (●), calcined SHTHPs (■) and the hollow material (▲) prepared by replacing ammonia with water. 1 C = 168 mA g^{-1}. (b) Cycling performance and Coulombic efficiency of calcined SHTHPs under a current rate of 1 C.

attributed to the low conductive of TiO_2. Owing to its special hierarchical structure, the spinous hollow titania material exhibited higher storage capacity than that of the solid titania material and hollow material prepared by replacing ammonia with water.[50-52] First of all, the nanobelts on the surface could shorten the diffusion length of Li^+, benefit for Li^+ insertion. Moreover, the hierarchical hollow structure with higher specific surface area could ensure the efficient contact between the electrode and electrolyte. Finally, the hollow micro-sized particles could help inhibit the aggregation of the primary nanoparticles. Fig.S7† showed the discharge-charge voltage curves of calcined SHTHPs. Two clear potential plateaus around 1.75 and 1.95 V were observed, corresponding to lithium-ion intercalation and deintercalation. As presented in Fig. 6b, the hollow material demonstrated well cycling performance. In the first cycles under a 1 C rate, the sample showed a discharge capacity of 225 mA h g^{-1}. A specific discharge capacity of 125 mA h g^{-1}can be retained after 40 cycles, approximately 56% of its initial discharge. During all the cycles, the Coulombic efficiency was maintained around 100% but for the first cycle of 80%,which might be related to the insulating character of titania and the side reactions, such as water molecules absorbed on the spinous surface of the calcined SHTHPs.[53]

Conclusions

In summary, hierarchical spinous hollow titania hexagonal prisms composed of ultrathin nanobelts have been successfully fabricated via a self-template route. Through a simple solvothermal treatment we could obtain a series of nanostructures with complicated morphologies, including core-shell, yolk-shell nanostructures. Ammonia could assist in the synthesis of the spinous microparticle surface consisting of numerous nanobelts and accelerate the conversion of the TC to titania. The final hollow material shows a high discharge capacity of 225 mA h g^{-1} in the first cycle at a current density of 168 mA g^{-1}. It is noteworthy that such a fluorine-free synthesis method with the involvement of the Kirkendall process is environmental-friendly, reproducible and effective for the design of advanced lithium-ion battery electrode materials. Moreover, this new special hollow structure is expected to have potential applications in photocatalyst, solar cell and gas sensing in the near future.

Acknowledgements

Notes and reference

^{a}StateKey Laboratory of Inorganic Synthesis and Preparative Chemistry, College of Chemistry, Jilin University, Changchun 130012; P. R. China. E-mail: huoqisheng@jlu.edu.cn; Tel: +86-431-85168602
^{b}Department of Mechanical and Nuclear Engineering,The Pennsylvania State University 272 Materials Research Laboratory, University Park, PA, 16802, USA.
†Electronic supplementary information (ESI) available.

1   X. W. Lou, L. A. Archer and Z. Yang, *Adv. Mater.*, 2008, 20, 3987-4019.

2   M. Chen, C. Ye, S. Zhou and L. Wu, *Adv. Mater.*, 2013, 25, 5343-5351.

3   B. Guan, T. Wang, S. Zeng, X. Wang, D. An, D. Wang, Y. Cao, D. Ma, Y. Liu and Q. Huo, *Nano Research*, 2014, 7, 246-262.

4   X. Han, L. Li and C. Wang, *Nanoscale*, 2013, 5, 7193.

5   Z. Wang, L. Zhou and X. W. David Lou, *Adv. Mater.*, 2012, 24, 1903-1911.

6   X. Ma, Y. Zhao, K. W. Ng and Y. Zhao, *Chem.-Eur. J.*, 2013, 19, 15593-15603.

7   S. Tang, X. Huang, X. Chen and N. Zheng, *Adv. Funct. Mater.*, 2010, 20, 2442-2447.

8   L. Zhou, Z. Chen, K. Dong, M. Yin, J. Ren and X. Qu, *Adv. Mater.*, 2014, 26, 2424-2430.

9   Y. Liu, J. Goebl and Y. Yin, *Chem. Soc. Rev.*, 2013, 42, 2610.

10 B. Guan, X. Wang, Y. Xiao, Y. Liu and Q. Huo, *Nanoscale*, 2013, 5, 2469.

11 X.-J. Wu and D. Xu, *Adv. Mater.*, 2010, 22, 1516-1520.

12 J. Liu, S. B. Hartono, Y. G. Jin, Z. Li, G. Q. Lu and S. Z. Qiao, *J. Mater. Chem.*, 2010, 20, 4595.

13 H. B. Wu, A. Pan, H. H. Hng and X. W. D. Lou, *Adv. Funct. Mater.*, 2013, 23, 5669-5674.

14 H. Xu and W. Wang, *Angew. Chem. Int. Ed.*, 2007, 46, 1489-1492.

15 Q. Zhang, W. Wang, J. Goebl and Y. Yin, *Nano Today*, 2009, 4, 494-507.

16 L. N. Paritskaya, *Defect and Diffusion Forum*, 2006, 249, 73-80.

17 Y. Yin, *Science*, 2004, 304, 711-714.

18 B. Liu and H. C. Zeng, *Small*, 2005, 1, 566-571.

19 X.-Y. Yu, X.-Z. Yao, T. Luo, Y. Jia, J.-H. Liu and X.-J. Huang, *ACS Appl. Mater. Interfaces*, 2014, 6, 3689-3695.

20 Q. Zhang, I. Lee, J. Ge, F. Zaera and Y. Yin, *Adv. Funct. Mater.*, 2010, 20, 2201-2214.

21 X. Xia, Y. Wang, A. Ruditskiy and Y. Xia, *Adv. Mater.*, 2013, 25, 6313-6333.

22 X. Chen and S. S. Mao, *Chem. Rev.*, 2007, 107, 2891-2959.

23 D. Chen and R. A. Caruso, *Adv. Funct. Mater.*, 2013, 23, 1356-1374.

24 H. Zhao, L. Liu, J. M. Andino and Y. Li, *J. Mater. Chem. A*, 2013, 1, 8209.

25 D. Chen, F. Huang, Y.-B. Cheng and R. A. Caruso, *Adv. Mater.*, 2009, 21, 2206-2210.

26 S. Liu, H. Jia, L. Han, J. Wang, P. Gao, D. Xu, J. Yang and S. Che, *Adv. Mater.*, 2012, 24, 3201-3204.

27 H. Wang, M. Miyauchi, Y. Ishikawa, A. Pyatenko, N. Koshizaki, Y. Li, L. Li, X. Li, Y. Bando and D. Golberg, *J. Am. Chem. Soc.*, 2011, 133, 19102-19109.

28 F. Huang, D. Chen, X. L. Zhang, R. A. Caruso and Y.-B. Cheng, *Adv. Funct. Mater.*, 2010, 20, 1301-1305.

29 D. Chen, F. Huang, L. Cao, Y.-B. Cheng and R. A. Caruso, *Chemistry – A European Journal*, 2012, 18, 13762-13769.

30 J. B. Joo, M. Dahl, N. Li, F. Zaera and Y. Yin, *Energy Environ. Sci.*, 2013, 6, 2082-2092.

31 X. Pan, M.-Q. Yang, X. Fu, N. Zhang and Y.-J. Xu, *Nanoscale*, 2013, 5, 3601-3614.

32 X. Wang, L. Cao, D. Chen and R. A. Caruso, *ACS Appl. Mater. Interfaces*, 2013, 5, 9421-9428.

33 J. Ye, W. Liu, J. Cai, S. Chen, X. Zhao, H. Zhou and L. Qi, *J. Am. Chem. Soc.*, 2011, 133, 933-940.

34 J.-Y. Shin, D. Samuelis and J. Maier, *Adv. Funct. Mater.*, 2011, 21, 3464-3472.

35 Y. Ma, G. Ji, B. Ding and J. Y. Lee, *J. Mater. Chem.*, 2012, 22, 24380.

36 S. Brutti, V. Gentili, H. Menard, B. Scrosati and P. G. Bruce, *Adv. Energy Mater.*, 2012, 2, 322-327.

37 Q. Deng, M. Wei, X. Ding, L. Jiang, B. Ye and K. Wei, *Chem. Commun.*, 2008, 3657.

38 Y. Wang, X. Su and S. Lu, *J. Mater. Chem.*, 2012, 22, 1969.

39 G. S. Zakharova, C. Jähne, A. Popa, C. Täschner, T. Gemming, A. Leonhardt, B. Büchner and R. Klingeler, *J. Phys. Chem. C*, 2012, 116, 8714-8720.

40 Y. Zhao, F. Pan, H. Li, D. Zhao, L. Liu, G. Q. Xu and W. Chen, *J. Phys. Chem. C*, 2013, 117, 21718-21723.

41 J. H. Pan, X. Z. Wang, Q. Huang, C. Shen, Z. Y. Koh, Q. Wang, A. Engel and D. W. Bahnemann, *Adv. Funct. Mater.*, 2014, 24, 95-104.

42 L. Cao, D. Chen and R. A. Caruso, *Angew. Chem. Int. Ed.*, 2013, 52, 10986-10991.

43 D. Wu, F. Zhu, J. Li, H. Dong, Q. Li, K. Jiang and D. Xu, *J. Mater. Chem.*, 2012, 22, 11665.

44 D. Dambournet, I. Belharouak and K. Amine, *Chem. Mater.*, 2010, 22, 1173-1179.

Nanoscale Accepted Manuscript

45 C. Boudaren, T. Bataille, J.-P. Auffrédic and D. Louër, *Solid State Sciences*, 2003, 5, 175-182.

46 C. Weidenthaler, *Nanoscale*, 2011, 3, 792-810.

47 R. Asahi, T. Morikawa, T. Ohwaki, K. Aoki and Y. Taga, *Science*, 2001, 293, 269-271.

48 J. X. Wang, C. Ma, Y. Choi, D. Su, Y. Zhu, P. Liu, R. Si, M. B. Vukmirovic, Y. Zhang and R. R. Adzic, *J. Am. Chem. Soc.*, 2011, 133, 13551-13557.

49 T. Sugimoto, K. Okada and H. Itoh, *J. Dispersion Sci. Technol.*, 1998, 19, 143-161.

50 A. Pan, H. B. Wu, L. Yu and X. W. Lou, *Angew. Chem. Int. Ed.*, 2013, 125, 2282-2286.

51 S.-T. Myung, N. Takahashi, S. Komaba, C. S. Yoon, Y.-K. Sun, K. Amine and H. Yashiro, *Adv. Funct. Mater.*, 2011, 21, 3231-3241.

52 V. Etacheri, Y. Kuo, A. Van der Ven and B. M. Bartlett, *J. Mater. Chem. A*, 2013, 1, 12028-12032.

53 G. F. Ortiz, I. Hanzu, T. Djenizian, P. Lavela, J. L. Tirado and P. Knauth, *Chem. Mater.*, 2008, 21, 63-67.